

# Pseudoelasticity and the Strain-Memory Effect in Cu-Zn-Sn Alloys

J. D. EISENWASSER AND L. C. BROWN

Pseudoelasticity and the strain-memory effect have been studied in alloys with compositions in the range Cu-33 to 35 wt pct Zn-3 to 3.5 wt pct Sn, having a retained  $\beta$  structure and a martensitic transformation below room temperature. The alloys show maximum pseudoelasticities of 8.5 pct for single crystals and 4.5 pct for polycrystals at temperatures close to  $A_f$ . In single crystals high elasticity is retained to at least 100°C above  $A_f$  but in polycrystals it decreases rapidly above  $A_f$ . The strain-memory effect occurs on deformation below  $M_s$  with subsequent heating between  $A_s$  and  $A_f$ . The two effects are complementary, such that when one is large the other is small and vice versa. The total pseudoelastic and strain-memory recoveries are normally close to 100 pct. Both effects can be explained on the basis of the formation of a particular variant of the martensite giving significant elongations to the specimens. For pseudoelasticity, the initial structure is the  $\beta$  phase and the oriented martensite reverts to the  $\beta$  phase on removal of the stress. In the strain-memory effect the initial structure is oriented thermal martensite and the oriented martensite disappears only on heating to between  $A_s$  and  $A_f$  so that the martensite reverts to the  $\beta$  matrix.

IN a recent paper, Pops<sup>1</sup> has shown that coarse-grained specimens of  $\beta$  Cu-Zn-Sn and Cu-Zn-Si can have high degrees of pseudoelasticity. In these alloys the high temperature  $\beta$  phase is retained on quenching with a martensite transformation occurring just below room temperature. On stressing at room temperature, the martensite becomes thermodynamically stable and gives large elongations to the specimen. On removal of the stress the martensite disappears and the specimen regains its original length, thus giving pseudoelastic behavior. Similar pseudoelastic effects have been reported in Cu-Al-Ni,<sup>2,3</sup> Au-Cd,<sup>4</sup> In-Tl,<sup>5</sup> and Ag-Cd.<sup>6</sup>

The strain-memory effect has not been specifically reported in the Cu-Zn-Sn system, but has been found in several analogous alloys, such as Au-Cd,<sup>7</sup> In-Tl,<sup>8</sup> Ti-Ni,<sup>9</sup> Ti-Nb,<sup>10</sup> Cu-Al-Ni,<sup>3,11</sup> and Cu-Zn.<sup>12</sup> In this effect, an alloy is deformed below  $M_s$  and shows complete recovery on heating to between  $A_s$  and  $A_f$ .

There is obviously a very close interrelationship between pseudoelasticity and the strain-memory effect and the purpose of this paper will be to discuss this in Cu-Zn-Sn alloys. The observations of Pops<sup>1</sup> will be extended to cover single crystals, with polycrystalline observations being discussed where they differ from single crystal ones.

## EXPERIMENTAL

Alloys were melted in evacuated quartz tubes using high purity copper (99.98 pct), zinc (99.999 pct), and tin (99.99 pct) and homogenized by annealing at 810°C for 24 hr.

Polycrystalline specimens were produced by hot roll-

ing at 810°C to a thickness of 0.045 in., and then cold rolling to 0.040 in.

Single crystals were grown by the standard Bridgman method. The previously cast billets were resealed in quartz tube and solidified at a rate of 5 cm per hr from a point to give a crystal of uncontrolled orientation but with a tendency to be moderately close to  $\langle 110 \rangle$ . Slices 0.040 in. thick were cut from the billets by spark machining.

Tensile specimens were produced from the single and polycrystalline strip by spark machining. They were solution treated at 810°C for 1 min and then quenched into 10 pct caustic soda solution to retain the  $\beta$  phase. The polycrystalline material had a grain size of 1 to 2 mm.

All tensile tests were carried out with an Instron machine at a cross-head speed of 0.005 in. per min and were corrected for machine compliance. Tests below room temperature were made in chilled ethyl alcohol. The strain-memory effect was studied by stressing a specimen and then unloading it at a fixed temperature. On warming up to a given temperature the load increased again and the strain required to bring the load back to zero gave a measure of the strain-memory recovery at that temperature.

Transformation temperatures were measured by visual observation of specimens cooled in ethyl alcohol. In general, etching was not required to observe the microstructure. Habit planes of the martensite were found by the standard two-surface method. For stress-induced martensite, specimens were strained in a small tensile device and the martensite traces were photographed on two surfaces at right angles to each other.

## RESULTS AND DISCUSSION

Typical stress-strain curves for single crystal specimens oriented close to  $[011]$  are shown in Fig. 1. The alloy had a composition of 62.3 wt pct Cu, 34.7 wt pct

J. D. EISENWASSER is Graduate Student, Department of Metallurgy, University of British Columbia, Vancouver, Canada. L. C. BROWN, currently on leave from the Department of Metallurgy, University of Melbourne, Victoria, Australia, is Associate Professor, Department of Metallurgy, University of British Columbia.

Manuscript submitted October 18, 1971.

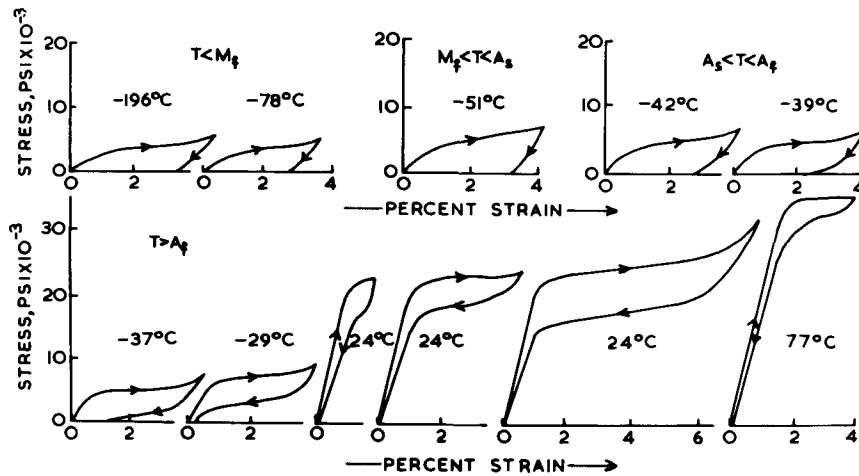
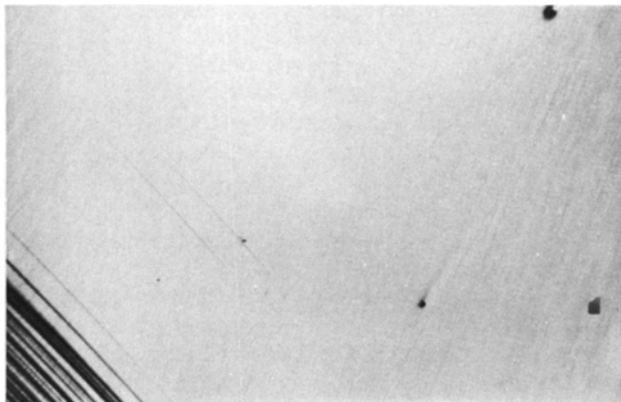
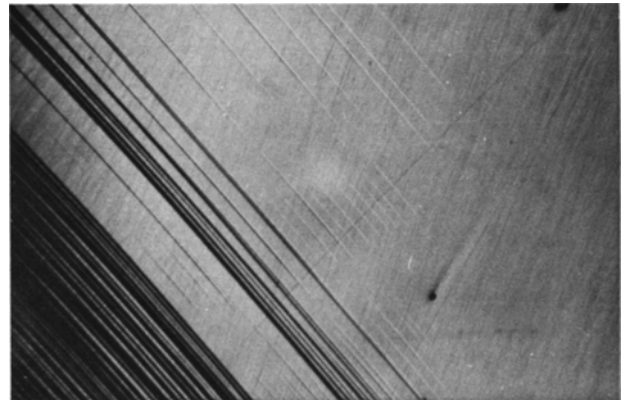


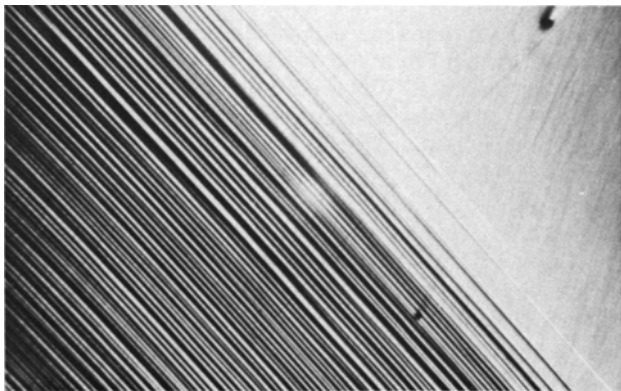
Fig. 1—Effect of temperature on the stress-strain curves for Cu-34.7 wt pct Zn-3.0 wt pct Sn single crystal specimens.



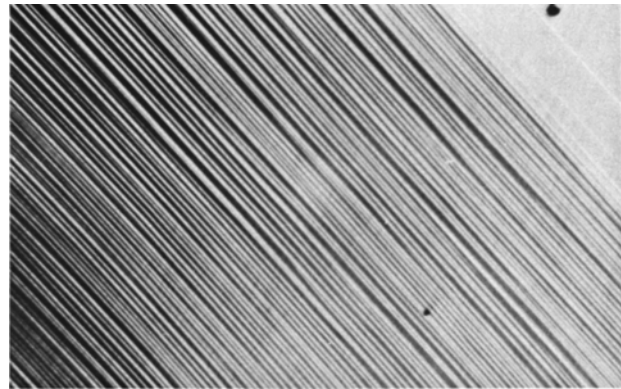
(a)



(b)



(c)



(d)

Fig. 2—Direct observations of SIM taken while stressing a single crystal. Magnification 35 times.

Zn, and 3.0 wt pct Sn and the following transformation temperatures:  $M_f = -65^\circ\text{C}$ ,  $M_s = -52^\circ\text{C}$ ,  $A_s = -50^\circ\text{C}$ , and  $A_f = -38^\circ\text{C}$ .

At temperatures above  $A_f$ , the stress-strain curves are very similar to those obtained by Pops and the specimens show very high degrees of elasticity (up to 9 pct). The initial linear portion of the tensile curve shows significant elasticity, varying from 0.5 pct strain at  $-31^\circ\text{C}$  to 1.55 pct strain at  $77^\circ\text{C}$ . These apparent elastic strain values are much larger than for a normal metal and can be explained as due to the very low strength of the  $\beta$  lattice to a  $\{110\}\langle 110\rangle$  shear. As discussed by Zener,<sup>13</sup> this low strength also gives rise to

a large increase in elastic modulus with temperature, in the present case from  $1 \times 10^6$  psi at  $-29^\circ\text{C}$  to  $2.3 \times 10^6$  psi at  $77^\circ\text{C}$ .

Most of the elasticity observed is associated with the plateau region of the stress-strain curve and this is due to stress-induced martensite (SIM) formation. Direct observations of the martensite show that it starts to form at the very beginning of the plateau region of the stress-strain curve, Fig. 2(a). It is in the form of very thin plates characteristic of thermoelastic martensite. With increasing strain, Figs. 2(b) to 2(d), more and more plates form across the specimen until at the end of the plateau portion transformation to martensite is complete and individual plates cannot be resolved. This gradual process of densification of mar-

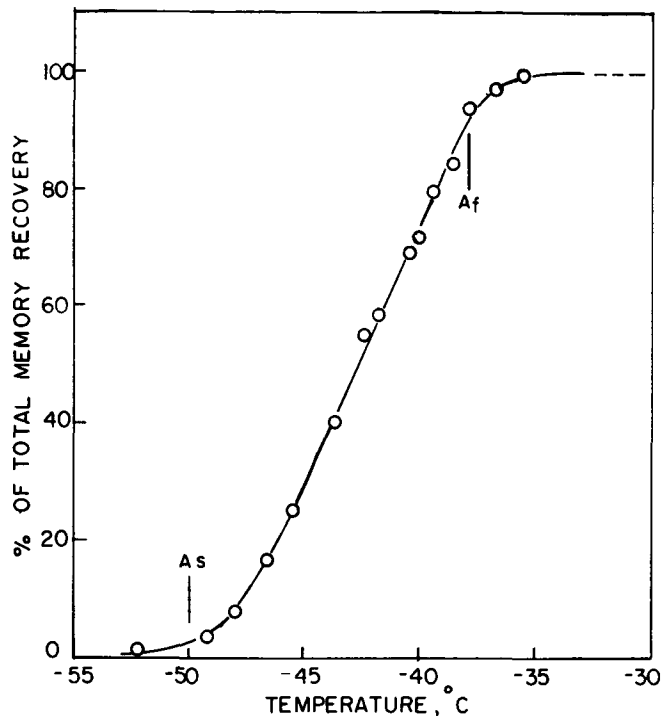


Fig. 3—Recovery of a single crystal specimen deformed at  $-69^{\circ}\text{C}$  and allowed to slowly warm up.

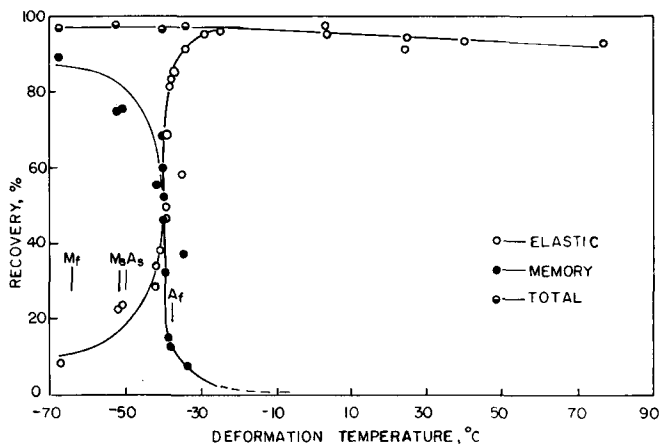


Fig. 4—Effect of deformation temperature on the elastic strain-memory recovery in single crystal specimens, showing almost complete recovery of strain.

tensite needles is quite different from the sudden formation of burst martensite observed in  $\text{Cu-Al-Ni}^3$  and results in much smoother stress-strain curves.

At temperatures below  $A_f$  the elasticity drops very rapidly. Above  $M_f$ , the stressing still causes formation of SIM but this is stable once formed and does not revert to the  $\beta$  phase on removal of the stress. Below  $M_f$  the structure is completely martensitic to start with and cannot show any SIM formation. Specimens still have a certain amount of elasticity, however, since the martensite structure will have a low resistance to shear just like the  $\beta$  matrix.

Specimens deformed below  $A_s$  show significant recovery when heated. Fig. 3 shows clearly that this recovery is associated with the transformation of the martensite to the  $\beta$  matrix, with recovery starting at  $A_s$  and being complete at  $A_f$ . Fig. 4 shows both the pseudoelastic and strain memory recoveries for speci-

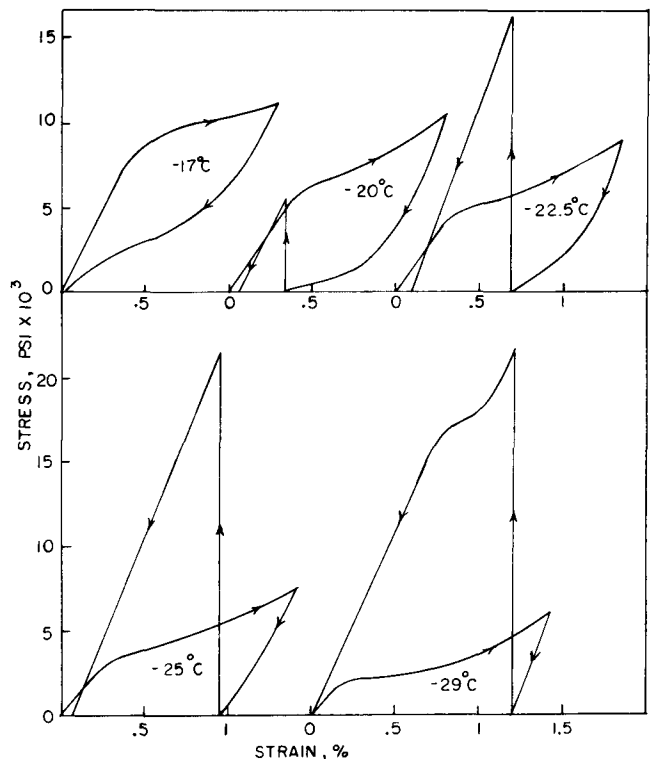


Fig. 5—Effect of temperature on the stress-strain curves for  $\text{Cu-33.3 wt pct Zn-3.2 wt pct Sn}$  polycrystalline specimens. The effect of heating the specimen to room temperature at constant strain and then releasing the load is also shown.

mens deformed at various temperatures and allowed to warm up to room temperature. The graph shows very clearly the relationship between the two effects—when one is large, the other is small. Total recovery is approximately 96 pct for all temperatures up to  $A_f$ . Above this it slowly decreases due to plastic deformation of the martensite owing to the increasing stress for SIM formation.

The pseudoelastic and strain-memory observations for polycrystalline specimens showed the same main features as for single crystals. The alloy used had a composition of  $\text{Cu-33.3 wt pct Zn-3.2 wt pct Sn}$  and the following transformation temperatures:  $M_f = -34^{\circ}\text{C}$ ,  $M_s = -27^{\circ}\text{C}$ ,  $A_s = -25^{\circ}\text{C}$ , and  $A_f = -14^{\circ}\text{C}$ . The stress-strain curves in Fig. 5 give the pseudoelasticity from the recovery on unloading at a fixed temperature. The strain-memory recovery is given by heating the specimen to above  $A_f$  at constant strain and then finding the strain recovered on release of the stress. As in single crystals, when one effect is large the other is small and the total recovery is at least 90 pct for temperatures up to  $A_f$ .

One of the major differences with polycrystals compared with single crystal tests was that the maximum amount of recovery was much less—4.5 pct strain compared with 8.5 pct strain for single crystals. This is due to the fact that when martensite forms it cannot extend right across the specimen but is restricted by the grain boundaries and plastic deformation occurs there at relatively early stages in the transformation. The other major difference is that in polycrystals the elastic recovery has a maximum close to  $A_f$  and decreases rapidly above this temperature, Fig. 6. The reason for this rapid decrease compared with single crystals is that at the high temperatures, the stress

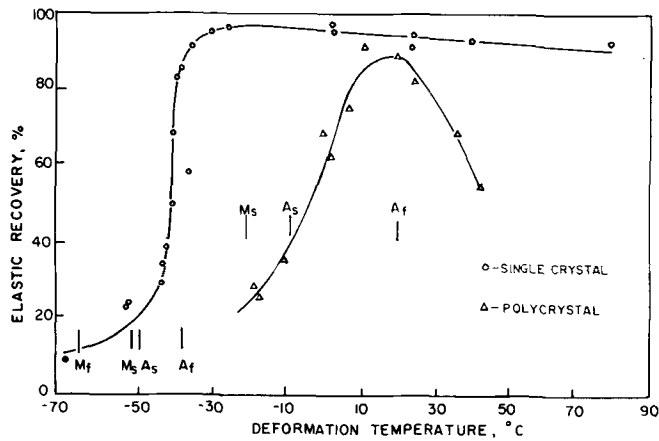


Fig. 6—Effect of temperature on the pseudoelastic recovery in single and polycrystalline specimens.

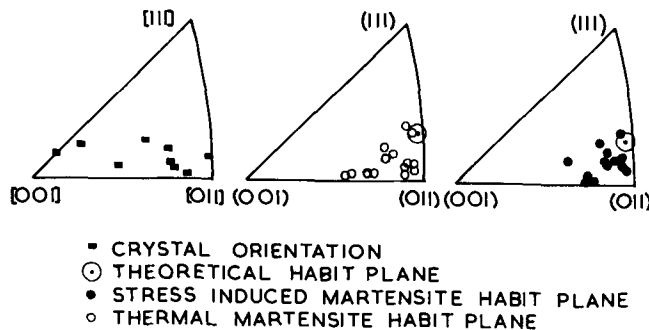


Fig. 7—Observed habit planes for thermal and stress-induced martensite together with the calculated plane from the WLR analysis.

required for nucleation of martensite inside the grains is sufficient to cause plastic deformation at the grain boundaries and so give nonrecoverable slip.

Habit planes for thermal stress-induced martensite were measured for several specimens as shown in Fig. 7. In all cases the habit plane was found to be close to  $\{110\}$ .

Ahlers and Pops<sup>14</sup> have applied the Wechsler-Liebermann-Read (WLR) theory<sup>15</sup> for thermal martensite to deformation martensite in Cu-Zn single crystals. They find that lattice-invariant shears of  $\{110\}\langle 110\rangle$  give habit planes close to  $\{110\}$  and in good agreement with experiment. A  $\{110\}\langle 110\rangle$  shear seems particularly probable owing to the low strength of the martensite in this direction. A similar calculation for the present alloy gives a habit plane in moderate agreement with the experimental data for a  $(110)[\bar{1}\bar{1}0]$  shear. The lattice parameters used for this calculation were  $a = 2.940\text{\AA}$  for the  $\beta$  phase and  $a = 2.678\text{\AA}$ ,  $b = 4.283\text{\AA}$ ,  $c = 4.474\text{\AA}$  for the orthorhombic martensite, with the Bain relationship  $[100]_{\beta} \parallel [010]_{\alpha}$  and  $[010]_{\beta} \parallel [\bar{1}\bar{1}0]_{\alpha}$ .<sup>16</sup> Other possible shears such as  $(011)[0\bar{1}\bar{1}]$ ,  $(\bar{1}\bar{1}\bar{1})[112]$  do not give nearly such good agreement with experiment.

The WLR theory also gives the magnitude and direction of the macroscopic shear associated with the formation of a martensite plate. In the present case the macroscopic shear is 0.1974 in the  $(0.8429, 0.2079, 0.4963)$  direction. As discussed by Krishnan and Brown,<sup>6</sup> the macroscopic shear during SIM formation is responsible for the specimen elongation. Martensite

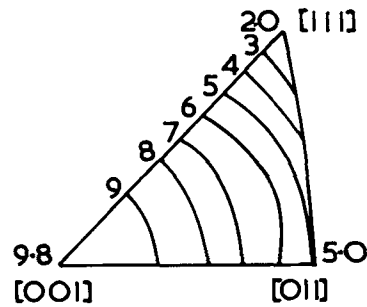


Fig. 8—Stereographic projection showing contours of equal strain obtained during SIM formation for various orientations of the tensile axis.

forms on the particular variant of the habit plane that is most favored by the applied stress. This variant is the one in which the shear component of the applied stress is a maximum in the direction of the macroscopic shear associated with the martensite transformation. The elongation associated with the particular variant can then be calculated from

$$\epsilon = \frac{1}{2} \sin 2\phi \tan \gamma \cos \alpha$$

where

$\phi$  is the angle between the habit plane normal and the tensile axis

$\alpha$  is the angle between the plane containing the habit plane normal and the tensile axis and the plane containing the habit plane normal and the tensile axis

$\tan \gamma$  is the macroscopic shear

All these quantities can be calculated from the WLR analysis. As shown in Fig. 8, the elongation is a function of specimen orientation, being very large close to  $[001]$  and decreasing progressively on moving away from this orientation. Apart from orientations close to  $[111]$  elongations associated with SIM formation correspond to at least 5 pct strain. To this must be added the apparent elastic elongation at the beginning of the stress-strain curve which can be as large as 1.5 pct strain. Hence the theory explains the observed pseudoelastic effect satisfactorily.

The strain-memory effect can be explained in the same manner. Martensite forms on cooling with negligible dimensional changes in the specimen ( $<0.1$  pct), provided it is under zero stress. This is because all variants of the martensite form and any elongation associated with one particular variant is cancelled out by one of the others. On stressing, however, one variant grows at the expense of the others so that ultimately only one orientation of martensite exists. The amount of strain associated with this change in the microstructure is given by Fig. 8. On release of the stress, the oriented martensite is unaffected except for the release of elastic strain. Only on heating to between  $A_s$  and  $A_f$  where the oriented martensite transforms to the  $\beta$  matrix is the strain recovered.

The present explanation for the strain-memory effect is different from the more common one which attributed it to a change in the internal structure of the thermal martensite with one twin orientation growing at the expense of the other to give the required

strain.<sup>11</sup> It is possible that stressing would cause a change in the stacking fault configuration in  $\beta$  Cu-Zn-Sn. However this would tend to cause a change in crystal structure and an explanation based on the growth of one variant at the expense of the others seems preferable.

### CONCLUSIONS

1) Single crystals of  $\beta$  Cu-Zn-Sn have maximum pseudoelastic strains of 8.5 pct, while polycrystalline specimens have maximum strains of 4.5 pct.

2) Single and polycrystalline specimens can have fairly large amounts of apparent elastic strain, in some cases up to 1.6 pct. This is due to the instability of the matrix and martensite structures to a  $\{110\}$   $\langle 110 \rangle$  shear.

3) The greatest fraction of the pseudoelasticity is associated with SIM formation and only occurs above  $A_s$ . In single crystals, pseudoelasticity is maintained to at least 100°C above  $A_f$ , while in polycrystals significant pseudoelasticity occurs only close to  $A_f$  with plastic deformation occurring at higher temperatures.

4) The strain-memory effect occurs on deformation below  $M_s$  and subsequent heating between  $A_s$  and  $A_f$ . There appears to be no lower limit to the deformation temperature below  $M_f$ .

5) There is a very close relationship between pseudoelasticity and the strain memory effect such that when one is small the other is large and vice versa. The total recovery—pseudoelastic plus strain-memory—is close to 100 pct except for polycrystals above  $A_s$ .

6) Both thermal martensite and SIM have habit planes close to  $\{110\}$ . This can be explained from the WLR theory assuming a lattice invariant shear of  $(110)$   $[\bar{1}\bar{1}0]$ . This corresponds to a stacking fault shear.

7) The macroscopic shear associated with the formation of a martensite plate is responsible for the elongation of the specimen on loading. Favorably oriented martensite plates give elongations of 9 pct for specimens having a  $\langle 001 \rangle$  tensile axis. Other orientations of the tensile axis give smaller elongations, but in general at least 5 pct.

8) In the pseudoelastic effect oriented martensite plates form from the  $\beta$  matrix while in the strain-memory effect the oriented martensite forms from unoriented thermal martensite. In both effects the elongations are similar and there is a very close relation between the two effects.

### ACKNOWLEDGMENT

The authors wish to thank Dr. R. V. Krishnan for helpful discussions. The authors also wish to thank the National Research Council of Canada for financial assistance in the form of grant A-2549.

### REFERENCES

1. H. Pops: *Met. Trans.*, 1970, vol. 1, p. 251.
2. W. A. Rachinger: *J. Aust. Inst. of Metals*, 1960, vol. 5, p. 114.
3. K. Oishi and L. C. Brown: *Met. Trans.*, 1971, vol. 2, p. 1971.
4. J. Intrater, L. C. Chang, and T. A. Read: *Phys. Rev.*, 1952, vol. 86, p. 598.
5. N. W. Burkart and T. A. Read: *Trans. AIME*, 1953, vol. 197, p. 1516.
6. R. V. Krishnan and L. C. Brown: unpublished work, Univ. of Brit. Col., 1971.
7. D. S. Lieberman, T. A. Read, and L. C. Chang: *Phys. Rev.*, 1951, vol. 82, p. 340.
8. Z. S. Basinski and J. W. Christian: *Acta Met.*, 1954, vol. 2, p. 148.
9. W. J. Beuhler and F. E. Wang: *Ocean Eng.*, 1968, vol. 1, p. 105.
10. C. Baker: *Metal Sci. J.*, 1971, vol. 5, p. 92.
11. K. Otsuka: *Jap. J. Appl. Phys.*, 1971, vol. 10, p. 571.
12. C. M. Wayman: *Scripta Met.*, 1971, vol. 5, p. 489.
13. C. Zener: *Phys. Rev.*, 1947, vol. 71, p. 846.
14. M. Ahlers and H. Pops: *Trans. TMS-AIME*, 1968, vol. 242, p. 1267.
15. M. S. Wechsler, D. S. Lieberman and T. A. Read: *Trans. AIME*, 1953, vol. 197, p. 1503.
16. W. Jolley and D. Hull: *J. Inst. Metals*, 1964, vol. 92, p. 129.